An accurate method to include lubrication forces in numerical simulations of dense stokesian suspensions

A. Lefebvre-Lepot[1], B. Merlet [2] † and T.N. Nguyen[2]

[1]CNRS – Ecole Polytechnique/CMAP, route de Saclay, 91128 PALAISEAU Cedex, France
[2]Ecole Polytechnique/CMAP, route de Saclay, 91128 PALAISEAU Cedex, France

(Received ?; revised ?; accepted ?. - To be entered by editorial office)

We consider fluid-particle solvers computing the hydrodynamic interactions between rigid spheres with prescribed velocities moving in a Stokes fluid. This work proposes a new method to deal with the singularities which occur when the distance between particles with different velocities is small. Such situations yield large hydrodynamic forces which are localized in narrow areas and are thus difficult to capture numerically. To treat this difficulty, we use the superposition principle to decompose the solution into regular and singular parts. The forces and torques generated by the singular parts are obtained by interpolating over a set of values computed off-line. Then, one can use any standard numerical method to obtain an accurate approximation of the forces and torques generated by the "regular" part of the data. Numerical tests show that this singular-regular decomposition method improves the accuracy of the (now standard) Stokesian Dynamics lubrication correction.

Key words: Authors should not enter keywords on the manuscript, as these must be chosen by the author during the online submission process and will then be added during the typesetting process (see http://journals.cambridge.org/data/relatedlink/jfm-keywords.pdf for the full list)

A large amount of research has been conducted these last years to develop numerical tools in order to study the motion of objects in suspension in a Stokes fluid (see *e.g.* Patankar *et al.* (2000) and references therein for finite element methods, Cichocki *et al.* (1994) or Yeo & Maxey (2010) and references therein for multipole decomposition methods). Such systems are used to model the sedimentation of particle suspensions. They are also well fitted to model nano-scale swimmers, such as sperm cells, swimming bacteria or unicellular algae. Motivation also comes from recent advances in creating artificial nano-scale swimmers designed to deliver medication from nano-sized medical devices — see e.g. Douglas *et al.* (2012) as an example of the biomedical engineering activity in this area. The present work is more precisely motivated by the numerical simulation of theoretical artificial swimmers made of a finite number of balls studied in Alouges *et al.* (2008); Lefebvre-Lepot & Merlet (2009) or Alouges *et al.* (2013).

We consider N identical rigid spherical particles suspended in a viscous fluid that fills the whole space. We neglect inertia and consider a Stokes flow with vanishing conditions at infinity. The data are the instantaneous velocities and angular velocities $(\boldsymbol{U}_i, \boldsymbol{\omega}_i)_{1\leqslant i\leqslant N}$ of the particles. These velocities provide boundary conditions to the Stokes

† Email address for correspondence: benoit.merlet@cmap.polytechnique.fr

flow in the fluid domain and we want to compute the hydrodynamic forces and torques $(\boldsymbol{F}_i, \boldsymbol{T}_i)_{1\leqslant i\leqslant N}$ generated by this flow on each particle. The well known difficulty in such numerical simulations is to take into account the singular lubrication forces exerted by the fluid remaining in the gap between close particles.
In Section 1, we introduce the model, describe the standard Stokesian Dynamics correction introduced in Durlofsky *et al.* (1987) to deal with lubrication in numerical simulations and discuss its accuracy. We show that this correction to treat the interactions between close particles requires an improvement in the presence of large forces. In Section 2, we introduce a singular-regular decomposition method which is close to the method of Sangani & Mo (1994). The main difference is the way the singular part of the forces and the velocity field is approximated. We present numerical experiments in Section 3 and compare our correction method to the standard correction of the Stokesian Dynamics. In particular, we show the good behavior of our method for the computation of the displacement of the 3-sphere swimmer introduced in Najafi & Golestanian (2004).

1. Spherical particles in a Stokes flow

1.1. *The model and its Integral formulation*

We consider N non-intersecting spherical solid particles $\mathbf{B}_1, \cdots, \mathbf{B}_N$ immersed in a viscous fluid. We denote by $\boldsymbol{r}_1, \cdots, \boldsymbol{r}_N$ the centers of the particles and for simplicity, we suppose that the particles have the same radius $\rho = 1$. The instantaneous translational and rotational velocities $\boldsymbol{U}_i$ and $\boldsymbol{\omega}_i$ of particle i are known. We suppose that the fluid is of infinite extent in the three directions and denote by $\Omega_f = \mathbf{R}^3 \setminus \cup \mathbf{B}_i$ the domain filled by the fluid. The fluid velocity $\boldsymbol{u}$ and the pressure p solve the Stokes equations in the fluid domain,

$$\nabla \cdot \sigma \;=\; 0 \;\text{ and }\; \nabla \cdot \boldsymbol{u} \;=\; 0 \text{ in } \Omega_f \tag{1.1}$$

where $\sigma = \left(\nabla \boldsymbol{u} + \nabla \boldsymbol{u}^T\right) - p\mathrm{Id}$ is the stress tensor in the fluid. Without loss of generality, the viscosity of the fluid has been chosen equal to 1. On the surfaces of the particles, we consider a no-slip condition,

$$\boldsymbol{u} \;=\; \boldsymbol{v}_i, \text{ on } \partial \mathbf{B}_i, \; i = 1, \cdots, N. \tag{1.2}$$

The velocities $\boldsymbol{v}_i$ correspond to the rigid displacements of the particles,

$$\boldsymbol{v}_i\left(\boldsymbol{r}\right) \;=\; \boldsymbol{U}_i + \boldsymbol{\omega}_i \times \left(\boldsymbol{r} - \boldsymbol{r}_i\right), \text{ for } \boldsymbol{r} \in \mathbf{R}^3, \; i = 1, \cdots, N. \tag{1.3}$$

Finally, we suppose that the fluid is at rest at infinity:

$$\boldsymbol{u}\left(\boldsymbol{r}\right) \to 0, \; p\left(\mathbf{r}\right) \to 0 \text{ as } \; \boldsymbol{r} \to +\infty. \tag{1.4}$$

The object of the present work is, $(\boldsymbol{U}_i, \boldsymbol{\omega}_i)_{1\leqslant i\leqslant N}$ being given, to compute accurate approximations of the total forces and total torques exerted by each particle on the fluid:

$$\boldsymbol{F}_j \;=\; \int_{\partial \mathbf{B}_j} \boldsymbol{f}_j(\boldsymbol{r})\, dS(\boldsymbol{r}), \qquad \boldsymbol{T}_j \;=\; \int_{\partial \mathbf{B}_j} \left(\boldsymbol{r} - \boldsymbol{r}_j\right) \times \boldsymbol{f}_j(\boldsymbol{r})\, dS(\boldsymbol{r}), \tag{1.5}$$

where $\boldsymbol{n}_j$ denotes the exterior unit normal to the particle $\mathbf{B}_j$ and $\boldsymbol{f}_j = -\sigma\, \boldsymbol{n}_j$ is the surface density of forces exerted on the fluid by the surface $\partial \mathbf{B}_j$.

By linearity of the Stokes equations and of formulas (1.5), we have in fact to approximate a linear operator, namely, the resistivity operator

$$R \;:\; (\boldsymbol{U}_i, \boldsymbol{\omega}_i)_{1\leqslant i\leqslant N} \in \left(\mathbf{R}^3\right)^{2N} \longmapsto (\boldsymbol{F}_j, \boldsymbol{T}_j)_{1\leqslant j\leqslant N} \in \left(\mathbf{R}^3\right)^{2N}.$$

which describes the hydrodynamic interactions between the particles.

Let us extend the fluid domain by assuming that the fluid also fills the interior of the particles: we set $\tilde{\Omega}_f := \mathbf{R}^3 \setminus \partial\mathbf{B}_i$. We also extend the class of prescribed velocities on $\partial\mathbf{B}_i$ by considering general boundary data $\boldsymbol{g}_i \ : \ \partial\mathbf{B}_i \to \mathbf{R}^3$ satisfying the constraint

$$\int_{\partial\mathbf{B}_i} \boldsymbol{g}_i \cdot \boldsymbol{n}_i \ = \ 0. \tag{1.6}$$

Given $(\boldsymbol{g}_1, \cdots, \boldsymbol{g}_N) \in \mathcal{H}_0^{1/2}$, we consider the solution $(\boldsymbol{u}, p)$ of the homogeneous Stokes equations in $\tilde{\Omega}_f$ with boundary conditions $\boldsymbol{u} = \boldsymbol{g}_i$ on $\partial\mathbf{B}_i$ for $i = 1, \cdots, N$†.Eventually, for $j = 1, \cdots, N$, we define $\tilde{\boldsymbol{f}}_j \in H_0^{-1/2}(\partial\mathbf{B}_j, \mathbf{R}^3)$ as

$$\tilde{\boldsymbol{f}}_j \ = \ (\sigma_{int} - \sigma_{ext})\boldsymbol{n}_j, \tag{1.7}$$

where σ_{ext} (σ_{int}) is the trace on $\partial\mathbf{B}_j$ of the stress tensor $\sigma = \left(\nabla\boldsymbol{u} + \nabla\boldsymbol{u}^T\right) - p\mathrm{Id}$ from the exterior (the interior) of ball $\mathbf{B}_j$. This defines a symmetric operator,

$$\mathcal{R} \ : \ (\boldsymbol{g}_1, \cdots, \boldsymbol{g}_N) \ \longmapsto \ (\tilde{\boldsymbol{f}}_1, \cdots, \tilde{\boldsymbol{f}}_N).$$

This operator is called the generalized resistivity operator. It associates to the boundary data $(\boldsymbol{g}_1, \cdots, \boldsymbol{g}_N)$ the densities of hydrodynamic forces $(\tilde{\boldsymbol{f}}_1, \cdots, \tilde{\boldsymbol{f}}_N)$ exerted by the spheres $\partial\mathbf{B}_1, \cdots, \partial\mathbf{B}_N$ on the fluid.

Now, for $j = 1, \cdots, N$, we define the total force and torque $\tilde{\boldsymbol{F}}_j$ and $\tilde{\boldsymbol{T}}_j$ exerted by $\partial\mathbf{B}_j$ as in (1.5). We easily check that the interior force density $\sigma_{int}\boldsymbol{n}_j$ does not contribute to $\tilde{\boldsymbol{F}}_j$ and $\tilde{\boldsymbol{T}}_j$ (this follows from the Stokes formula and the fact that σ is a symmetric and divergence free tensor).

Consequently, for $(\boldsymbol{g}_1, \cdots, \boldsymbol{g}_N) = (\boldsymbol{v}_1, \cdots, \boldsymbol{v}_N)$, we have $(\tilde{\boldsymbol{F}}_j, \tilde{\boldsymbol{T}}_j) = (\boldsymbol{F}_j, \boldsymbol{T}_j)$ and the resistivity operator R writes $R \ = \ \Pi\,\mathcal{R}\,\Pi$, where Π denotes the projection on the space of rigid velocities:

$$\left\{(\boldsymbol{U}_1 + \boldsymbol{\omega}_1 \times (\boldsymbol{r} - \boldsymbol{r}_1), \cdots, \boldsymbol{U}_N + \boldsymbol{\omega}_N \times (\boldsymbol{r} - \boldsymbol{r}_N)) \ : \ \boldsymbol{U}_1, \cdots, \boldsymbol{U}_N, \boldsymbol{\omega}_1, \cdots, \boldsymbol{\omega}_N \in \mathbf{R}^3\right\}.$$

The advantage of the extension of the fluid domain appears when we consider the inverse $\mathcal{M} = \mathcal{R}^{-1}$ of the generalized resistivity operator. Indeed, the velocity field $\boldsymbol{u}$ solves the non-homogeneous Stokes equations in $\mathbf{R}^3$ with a surface source term located on $\partial\mathbf{B}_1, \cdots, \partial\mathbf{B}_N$ with densities $\tilde{\boldsymbol{f}}_1, \cdots, \tilde{\boldsymbol{f}}_N$. This velocity field is obtained by convolution of the sources with the Stokeslet

$$\boldsymbol{G}(\boldsymbol{r}) \ := \ \frac{1}{8\pi r}\left(\frac{1}{r}\mathrm{Id} + e_{\boldsymbol{r}} \otimes e_{\boldsymbol{r}}\right).$$

This explicit formula for the operator $\mathcal{M}$ is at the basis of boundary element methods. It is also the heart of the spectral discretization we used to test the different correction methods in our numerical experiments. In short, this method consists in computing a projection $\mathcal{M}^L$ of the approximate generalized mobility operator $\mathcal{M}$ on a finite dimensional basis made of the Vectorial Spherical Harmonics of order $l \leqslant L$. In a second step, we obtain an approximate resistivity matrix by computing $R^L := \Pi(\mathcal{M}^L)^{-1}\Pi$. In the sequel this method is called the *direct method* (a precise description can be found in Cichocki *et al.* (1994) for example). Note that the lubrication correction method we propose can be easily adapted to any other fluid-particle solver.

† To uniquely determine the pressure, we impose for example $\int_{\mathbf{B}_i} p = 0$ for $i = 1, \cdots, N$.

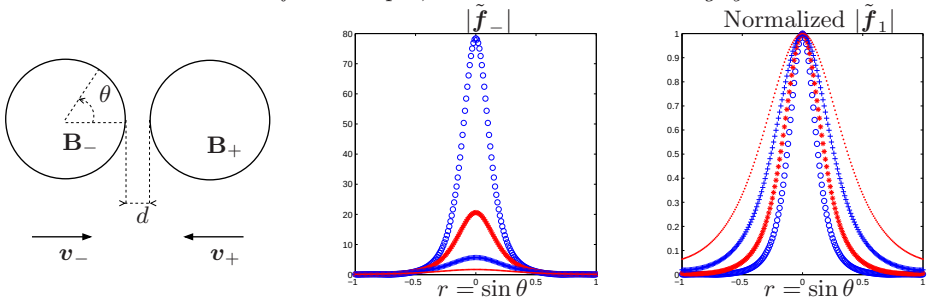

FIGURE 1. Pair of close spheres. Notations (left) and magnitude of the force density near the (almost) contact point on ∂B_- for various distances (middle and right). $d = 2.10^{-2}$ ($\circ\circ\circ$), $d = 4.10^{-2}$ ($\star\star\star$), $d = 8.10^{-2}$ ($+++$) and $d = 16.10^{-2}$ ($\cdots$).

1.2. *The Stokesian Dynamics correction for close particles*

As a spectral method, the direct method leads to an exponential convergence rate of R^L towards the exact resistivity matrix R for any given position of the particles. However, the method degenerates as the minimal distance between particles goes to 0. Indeed, when some particles are almost in contact, the possible discrepancy between the prescribed velocities on both sides of the thin gaps between particles leads to large magnitudes of $\nabla \boldsymbol{u}$. This phenomena combines with the incompressibility constraint to generate large lubrication forces with force densities located in small areas. More precisely, let us consider two isolated spheres $\mathbf{B}_-$, $\mathbf{B}_+$ with centers on the x axis separated by some (small) distance d, *i.e.* $\boldsymbol{r}_\pm = \pm(1 + d/2, 0, 0)$ (see Figure 1). We rewrite the prescribed velocities $\boldsymbol{v}_\pm(\boldsymbol{r}) = \boldsymbol{U}_\pm + \boldsymbol{\omega}_\pm \times (\boldsymbol{r} - \boldsymbol{r}_\pm)$ on $\partial\mathbf{B}_\pm$ as

$$\boldsymbol{v}_i \;=\; \boldsymbol{v}^{rig} + \boldsymbol{v}_i^{lub} \qquad \text{for } i = \text{`+'} \text{ and } i = \text{`}-\text{'}, \tag{1.8}$$

where $\boldsymbol{v}^{rig}$ is an instantaneous rigid motion of the solid $\mathbf{B}_- \cup \mathbf{B}_+$ and the two rest terms $\boldsymbol{v}_-^{lub}$, $\boldsymbol{v}_+^{lub}$ correspond to opposite rigid motions of $\mathbf{B}_-$ and $\mathbf{B}_+$. More precisely, we set

$$\boldsymbol{v}^{rig}(\boldsymbol{r}) = \bar{\boldsymbol{U}} + \bar{\boldsymbol{\omega}} \times \boldsymbol{r} \qquad \text{with} \qquad \bar{\boldsymbol{U}} := \frac{1}{2}\left(\boldsymbol{U}_- + \boldsymbol{U}_+\right), \quad \bar{\boldsymbol{\omega}} := \frac{1}{2}\left(\boldsymbol{\omega}_- + \boldsymbol{\omega}_+\right), \tag{1.9}$$

$$\boldsymbol{v}_-^{lub}(\boldsymbol{r}) = \hat{\boldsymbol{U}} + \hat{\boldsymbol{\omega}} \times (\boldsymbol{r} - \boldsymbol{r}_-), \qquad \boldsymbol{v}_+^{lub}(\boldsymbol{r}) = -\hat{\boldsymbol{U}} - \hat{\boldsymbol{\omega}} \times (\boldsymbol{r} - \boldsymbol{r}_+) \tag{1.10}$$

$$\text{with} \qquad \hat{\boldsymbol{U}} := \frac{1}{2}\left[\boldsymbol{U}_- - \boldsymbol{U}_+ + \bar{\omega} \times (\boldsymbol{r}_+ - \boldsymbol{r}_-)\right], \quad \hat{\boldsymbol{\omega}} := \frac{1}{2}\left(\boldsymbol{\omega}_- - \boldsymbol{\omega}_+\right).$$

The total force and torque $(\boldsymbol{F}_-, \boldsymbol{T}_-)$ then expand as follows as d goes to 0 — see Cox (1974).

$$F_{-,1} \;=\; 3\pi \hat{U}_1 d^{-1} + O(\ln d), \quad F_{-,m} \;=\; 2\pi \hat{U}_m \ln d + O(1) \text{ for } m = 2, 3. \tag{1.11}$$

$$\boldsymbol{T}_- \;=\; (0,\, -2\pi \hat{U}_3 + 6\pi/5\, \hat{\omega}_2\,,\, 2\pi \hat{U}_2 + 6\pi/5\, \hat{\omega}_3) \ln d + O(1). \tag{1.12}$$

These large total forces correspond to force densities concentrated in spherical caps with typical radius $O(\sqrt{d})$. This is illustrated by Figure 1 in the more singular case $\boldsymbol{U}_\pm = \mp(1, 0, 0)$: the magnitude of the force densities exerted by $\partial\mathbf{B}_-$ are displayed for different values of d. For such localized densities, a large number of degrees of freedom ($n_{dof} \gg 1/d$) is required in order to capture the relevant phenomenon (very fine meshes for finite element methods). For the spectral discretization of the direct method, this corresponds to a truncation order satisfying $L \gg 1/\sqrt{d}$.

To avoid using such costly simulations, the idea proposed in Durlofsky *et al.* (1987) for the Stokesian Dynamics is to correct the resistivity matrix by using exact values of

the hydrodynamic interactions between each pair of close balls. Let us briefly present this method. We first introduce a cut-off distance $\delta > 0$. Denoting by $d_{i,j}$ the distance between the particles $\mathbf{B}_i$ and $\mathbf{B}_j$, the set of pairs of close particles is defined as

$$\mathcal{P} \;:=\; \{(i,j) \;:\; 1 \leqslant i < j \leqslant N,\; d_{i,j} < \delta\}\,. \tag{1.13}$$

Now, if R^L is the approximation of R computed thanks to the direct method with a truncation order L, then the corresponding Stokesian Dynamics approximation of R is given by the formula

$$\mathsf{R}^L_{SD} \;=\; \mathsf{R}^L + \sum_{(i,j)\in\mathcal{P}} \big(\mathsf{R}_{i,j} - \mathsf{R}^L_{i,j}\big)\,. \tag{1.14}$$

The correction $\mathsf{R}_{i,j}$ is the exact resistivity operator (or a very accurate approximation) describing the interactions between the close particles $\mathbf{B}_i$ and $\mathbf{B}_j$ seen as an isolated pair. The last term $\mathsf{R}^L_{i,j}$ is the poor rank L approximation of these interactions which was already present in R^L and has to be substracted. This correction of the lubrication forces has been largely used for suspension simulations (see e.g. Brady & Bossis (1988); Ladd (1988); Cichocki *et al.* (1994)) and a modified method to compute the lubrication corrections $\mathsf{R}_{i,j}$ and $\mathsf{R}^L_{i,j}$ has also been proposed in Cichocki *et al.* (1999).

The correction (1.14) is very efficient and accurate in many cases of interest. However, it only concerns pairs of close particles: a third particle in the neighborhood of a pair of close particles is not affected by this correction. Let us assess the remaining error on a toy model. We consider a system of three particles $\mathbf{B}_1$, $\mathbf{B}_2$, $\mathbf{B}_3$ with centers on the x-axis and such that $\boldsymbol{r}_2 = \boldsymbol{r}_1 + (2+d)\mathbf{e}_x$ and $\boldsymbol{r}_3 = \boldsymbol{r}_2 + (2+D)\mathbf{e}_x$, so that $d_{1,2} = d$ with $0 < d < \delta$ and $d_{2,3} = D = O(1)$. Let us consider the two dimensional space $E = \langle b_1, b_2\rangle$ generated by $b_1 := (\boldsymbol{v}_1 = -\mathbf{e}_x, \boldsymbol{v}_2 = \mathbf{e}_x, \boldsymbol{v}_3 = 0)$ and $b_2 = (\boldsymbol{v}_1 = 0, \boldsymbol{v}_2 = 0, \boldsymbol{v}_3 = \mathbf{e}_x)$ and let us assume for simplicity that E is stable by $\mathcal{R}$. The projections of the resistivity and mobility operators on E have the form

$$R_{toy} \;=\; 3\begin{pmatrix} 1/(4d) & a \\ a & 1 \end{pmatrix}, \qquad M_{toy} \;=\; \frac{1}{3(1-4da^2)}\begin{pmatrix} 4d & -4da \\ -4da & 1 \end{pmatrix},$$

where $a = O(1)$ depends on D. Now, assume that on one hand, the truncation order L is sufficient to obtain an accurate approximation of the interactions between $\mathbf{B}_3$ and the pair $\mathbf{B}_1, \mathbf{B}_2$ and of the self-interactions of $\mathbf{B}_3$ but that on the other hand $L \lesssim 1/d$ so that we have a poor approximation of the lubrication forces between $\mathbf{B}_1$ and $\mathbf{B}_2$. Under these assumptions, we obtain an approximate mobility matrix of the form

$$M^L_{toy} \;=\; \frac{1}{3(1-4da^2)}\begin{pmatrix} 4d/\lambda & -4da \\ -4da & 1 \end{pmatrix}, \qquad \text{with } \lambda \in (0,1).$$

The corresponding approximation $R^L_{toy} := (M^L_{toy})^{-1}$ of the reduced mobility operator satisfies

$$R^L_{toy} \;=\; 3\frac{1-4da^2}{1-4\lambda da^2}\begin{pmatrix} \lambda/(4d) & \lambda a \\ \lambda a & 1 \end{pmatrix} \;=\; R_{toy} + \begin{pmatrix} O(1/d) & O(1) \\ O(1) & O(d) \end{pmatrix}.$$

The correction (1.14) eliminates the leading order term $O(1/d)$ of the error but does not affect the non-diagonal $O(1)$ error terms. The influence of the remaining error has negligible influence when we consider relatively small hydrodynamic forces. Indeed, in such cases, close particles have nearly identical velocities to avoid large lubrication forces. On the other hand, the correction (1.14) may be inadequate when hydrodynamic forces have to balance large non-hydrodynamic forces as it happens when we consider nano-

scale swimmers. In these cases, there is a need for numerical methods which are accurate even in the presence of large forces. We present such a method in the next section.

2. The singular-regular decomposition method

We propose to split the solution $(\boldsymbol{u}, p)$ of (1.1,1.2) into a singular part $(\boldsymbol{u}^{lub}, p^{lub})$ which contains the short range lubrication interactions and a regular remaining part $(\boldsymbol{u}^0, p^0)$. More precisely, we will decompose the velocity field as,

$$(\boldsymbol{u}, p) \;=\; (\boldsymbol{u}^0, p^0) + (\boldsymbol{u}^{lub}, p^{lub}) \qquad \text{with} \qquad (\boldsymbol{u}^{lub}, p^{lub}) \;=\; \sum_{(i,j)\in\mathcal{P}} (\boldsymbol{u}^{(i,j)}, p^{(i,j)}). \quad (2.1)$$

For $(i,j) \in \mathcal{P}$, the couple $\left(\boldsymbol{u}^{(i,j)}, p^{(i,j)}\right)$ handle the large variations of $(\boldsymbol{u}, p)$ localized in the small gap between $\mathbf{B}_i$ and $\mathbf{B}_j$ which are due to the difference between the prescribed velocities on $\partial\mathbf{B}_i$ and $\partial\mathbf{B}_j$. We obtain the singular part of the solution $\left(\boldsymbol{u}^{lub}, p^{lub}\right)$ by interpolating into tables computed off-line. The regular remaining part $\left(\boldsymbol{u}^0, p^0\right)$ can be computed by using any standard numerical method with a reasonable number of degrees of freedom. As already mentioned in the introduction, such a decomposition was proposed in Sangani & Mo (1994), where the singular part of the velocity and pressure fields was approximated using an asymptotic development of the solution up to a fixed order. Here, we propose a numerical method to compute these fields which allows us to reach any given precision by making the numerical parameters go to infinity.

Let us define more precisely the singular fields $(\boldsymbol{u}^{(i,j)}, p^{(i,j)})$. We first fix a cut-off distance $\delta > 0$ and define the set of close pairs of particles $\mathcal{P}$ as in (1.13). Now, for every pair $(i,j) \in \mathcal{P}$, we decompose the given velocity field on $\partial\mathbf{B}_i$ and $\partial\mathbf{B}_j$ according to (1.8,1.9,1.10)†. We obtain the decomposition,

$$\boldsymbol{v}_k \;=\; \boldsymbol{v}^{rig;(i,j)} + \boldsymbol{v}_k^{lub;(i,j)} \qquad \text{for } k = i, j.$$

Then, we consider the fictitious fluid domain $\Omega_f^{(i,j)} := \mathbf{R}^3 \setminus (\mathbf{B}_i \cup \mathbf{B}_j)$, (i.e. we replace the particles $\mathbf{B}_k$, $k \notin \{i,j\}$ with fluid). The "singular" field $\left(\boldsymbol{u}^{(i,j)}, p^{(i,j)}\right)$ is defined as the unique solution of the problem

$$\left.\begin{aligned} \nabla\cdot\sigma^{(i,j)} \;=\; 0, \qquad \nabla\cdot\boldsymbol{u}^{(i,j)} \;=\; 0 \quad \text{in } \Omega_f^{(i,j)}, \qquad (\boldsymbol{u}^{(i,j)}, p^{(i,j)})(\boldsymbol{r}) \;\overset{r\uparrow\infty}{\longrightarrow}\; 0. \\ \boldsymbol{u}^{(i,j)} \;=\; \boldsymbol{v}_k^{lub;(i,j)} \quad \text{on } \partial\mathbf{B}_k \quad \text{for } k = i, j. \end{aligned}\right\} \quad (2.2)$$

By linearity, (1.1,1.2,1.4) together with (2.2) implies that the remaining part $\left(\boldsymbol{u}^0, p^0\right)$ in (2.1) solves the following Stokes problem in Ω_f:

$$\left.\begin{aligned} \nabla\cdot\sigma^0 \;=\; 0, \qquad \nabla\cdot\boldsymbol{u}^0 \;=\; 0 \quad \text{in } \Omega_f, \qquad (\boldsymbol{u}^0, p^0)(\boldsymbol{r}) \;\overset{r\uparrow\infty}{\longrightarrow}\; 0. \\ \boldsymbol{u}^0 \;= \boldsymbol{v}_i^0 \quad \text{on } \partial\mathbf{B}_i, \quad \text{for } i = 1, \cdots, N. \end{aligned}\right\} \quad (2.3)$$

The new boundary condition $\boldsymbol{v}^0$ being given by

$$\boldsymbol{v}_i^0(\mathbf{r}) \;:=\; \boldsymbol{v}_i(\mathbf{r}) - \sum_{(k,l)\in\mathcal{P}} \boldsymbol{u}^{(k,l)}(\mathbf{r}), \text{ for } \mathbf{r} \in \partial\mathbf{B}_i, \; i = 1, \cdots, N. \quad (2.4)$$

Notice that for $(k,l) \in \mathcal{P}$ and $i \notin \{k,l\}$, the velocity field $\boldsymbol{u}^{(k,l)}$ does not correspond

† Of course, we proceed to a change of coordinates to transport the centers of $\mathbf{B}_i$ and $\mathbf{B}_j$ on the x-axis.

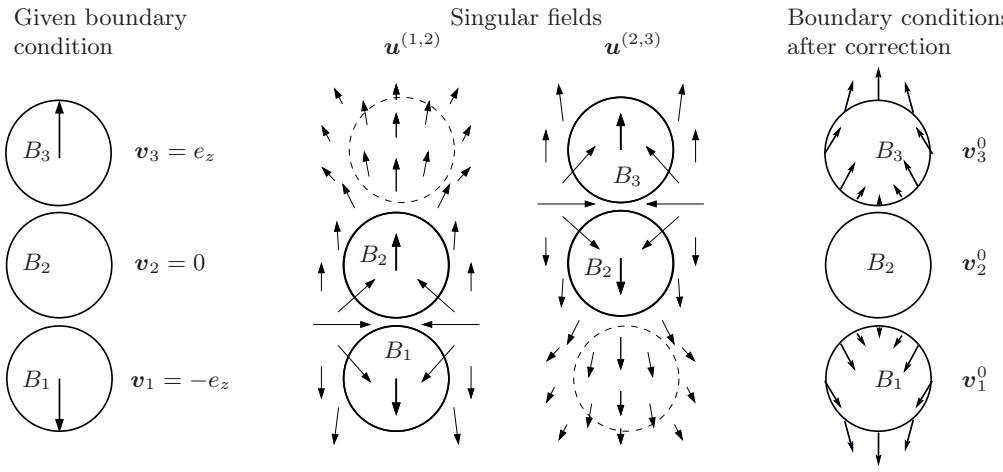

FIGURE 2. Example of decomposition in singular and regular parts.

to an instantaneous rigid motion and in general, the velocity field $\boldsymbol{v}_i^0$ does not have the simple structure (1.3). On the other hand, the velocity field $\boldsymbol{u}^{(k,l)}$ is uniformly smooth away from the contact point $\frac{1}{2}(\boldsymbol{r}_k + \boldsymbol{r}_l)$ and after the corrections (2.4) the new boundary conditions $\boldsymbol{v}_i^0$ do not create large localized force densities — see the example of Figure 2. Therefore we only need a small number of degrees of freedom to solve problem (2.3).

Let us now come back to our initial problem: $(\boldsymbol{U}_i, \boldsymbol{\omega}_i)_i$ being given, compute the forces $(\boldsymbol{F}_j)_j$ and torques $(\boldsymbol{T}_j)_j$ exerted on each particle and given by (1.5). Suppose that $\boldsymbol{u}^0$ and $\boldsymbol{u}^{(i,j)}$ for $(i,j) \in \mathcal{P}$ have been computed using any available method. Then, by linearity, we have with obvious notation,

$$\boldsymbol{F}_k \;=\; \boldsymbol{F}_k^0 + \sum_{(i,j)\in\mathcal{P}} \boldsymbol{F}_k^{(i,j)}, \quad \boldsymbol{T}_k \;=\; \boldsymbol{T}_k^0 + \sum_{(i,j)\in\mathcal{P}} \boldsymbol{T}_k^{(i,j)} \qquad \text{for } k = 1, \cdots, N. \tag{2.5}$$

In fact, in the above formulas, we only need to sum the terms $\boldsymbol{F}_k^{(i,j)}$, $\boldsymbol{T}_k^{(i,j)}$ over the subset $\{(i,j) \in \mathcal{P} \;:\; k \in \{i,j\}\}$. Indeed, for $(i,j) \in \mathcal{P}$, $k \notin \{i,j\}$ we have $\mathbf{B}_k \subset \Omega_f^{(i,j)}$ so that by the Stokes formula $\boldsymbol{F}_k^{(i,j)} = \boldsymbol{T}_k^{(i,j)} = 0$.

To conclude, this section, let us describe the way we have implemented the singular-regular decomposition method.

First, for the computation of the regular field $\boldsymbol{u}^0$, we have used a discretization of the integral formulation based on a decomposition of the data and unknowns in Vectorial Spherical Harmonics — *i.e.* we used the *direct method* cited in Section 1.1.

Next, the singular velocity fields $\boldsymbol{u}^{(i,j)}$ and the contributions $\boldsymbol{F}_k^{(i,j)}$, $\boldsymbol{T}_k^{(i,j)}$ for $(i,j) \in \mathcal{P}$ and $k = i, j$ are obtained by interpolation with respect to the parameter $d_{i,j} = d$ into tables computed off-line. More precisely, up to a change of coordinates we can assume that $\mathbf{B}_i = \mathbf{B}_-$ and $\mathbf{B}_j = \mathbf{B}_+$ where $\mathbf{B}_-$, $\mathbf{B}_+$ are the balls centered on the x-axis introduced in Section 1.2 with $d = d_{i,j}$. We now use the notation of Section 1.2 and we identify $\mathbf{B}_i$ with $\mathbf{B}_-$, $\mathbf{B}_j$ with $\mathbf{B}_+$, $\boldsymbol{u}^{(i,j)}$ with $\boldsymbol{u}^{(+,-)}$, $\boldsymbol{v}_i$ with $\boldsymbol{v}_-$, *etc.* In view of (1.10) the boundary conditions $\boldsymbol{v}_\pm^{lub}$ depend on the two vectors $\hat{\boldsymbol{U}}$ and $\hat{\boldsymbol{\omega}}$. We decompose these vectors as,

$$\hat{\boldsymbol{U}} \;=\; \alpha_1 \mathbf{e}_x + \alpha_2 \mathbf{e}, \qquad \hat{\boldsymbol{\omega}} \;=\; \alpha_3 \mathbf{e}_x + \alpha_4 \mathbf{e}',$$

where $\mathbf{e}$ and $\mathbf{e}'$ are unit vectors of the plane $\mathbf{e}_x^\perp$ and $\alpha_1, \alpha_2, \alpha_3, \alpha_4 \in \mathbf{R}$. By linearity

and using the symmetry of the problem with respect to rotations around the x-axis, the singular velocity field and the total force and torque exerted by $\partial\mathbf{B}_-$ and $\partial\mathbf{B}_+$ on the fluid have the form,

$$\begin{aligned} \boldsymbol{u}^{(+,-)}(\boldsymbol{r}) &= \textstyle\sum_{q=1}^4 \alpha_q \boldsymbol{u}_{sing.,q}(d,\boldsymbol{r}), \qquad \text{for } \boldsymbol{r}\in\mathbf{R}^3\setminus(\mathbf{B}_-\cup\mathbf{B}_+),\\ \boldsymbol{F}_\pm &= \pm\alpha_1 G_1(d)\mathbf{e}_x \pm \alpha_2 G_2(d)\mathbf{e}, \qquad \boldsymbol{T}_\pm = \alpha_2 S_2(d)\mathbf{e} \pm \alpha_3 S_3(d)\mathbf{e}_x \pm \alpha_4 S_4(d)\mathbf{e}', \end{aligned}$$

where $\boldsymbol{u}_{sing.,q}$ is the singular velocity field corresponding to coefficient α_q. For example, $\boldsymbol{u}_{sing.,1}$ is the solution to (2.2) where $\boldsymbol{v}_\pm^{lub}$ is given by (1.10) for $\hat{\boldsymbol{U}} = \mathbf{e}_x$ and $\hat{\boldsymbol{\omega}} = 0$. Hence, we need accurate approximations of the four velocity fields $\boldsymbol{u}_{sing.,q}(d,\boldsymbol{r})$ and of the five functions G_1, G_2, S_2, S_3, S_4. Let us start with the latter. In fact, from the expansions (1.11,1.12), we know that for $X\in\{G_1,G_2,S_2,S_3,S_4\}$, we have

$$X(d) = c_{X,1}\frac{1}{d} + c_{X,2}\ln d + c_{X,3} + \cdots,$$

where the leading order terms $X^{lead.}(d)$ in these expansions are explicitly known. Our problem boils down to obtain accurate approximations of the functions $R_X(d) := X(d) - X^{lead.}(d)$. To do this, we have used the direct method to compute accurate approximations of $\boldsymbol{F}_\pm$ and $\boldsymbol{T}_\pm$ for d ranging over a fine grid $d_h\in\mathcal{G} := \{10^{-3},\cdots,1/2\}$. Our approximation of $X(d)$ is then $X^{lead.}(d) + \tilde{R}_X(d)$, where $\tilde{R}_X(d)$ is the cubic spline interpolation of the values of $R_X(d_h)$, $d_h\in\mathcal{G}$ which have been computed off-line.
For the singular velocity fields, we have to chose a compact representation of the mappings $\boldsymbol{r}\mapsto\boldsymbol{u}_{sing.,q}(d,\boldsymbol{r})$,

$$\boldsymbol{u}_{sing.,q}(d,\boldsymbol{r}) = \sum_{n=1}^{n_{max}} H_q^n(d)\phi^n(\boldsymbol{r}),$$

and then build tables of the coefficients $H_q^n(d_h)$, for $d_h\in\mathcal{G}$. For the numerical experiments below, we use the fact that $\boldsymbol{u}_{sing.,q}$ solves the Stokes equations in $\mathbf{R}^3\setminus\mathbf{B}$ where $\mathbf{B}$ is the smallest ball centered at 0 which contains $\mathbf{B}_-\cup\mathbf{B}_+$. Hence, we can use a multipole decomposition of $\boldsymbol{u}_{sing.,q}(d,\boldsymbol{r})$. As above, we have used the direct method to build the tables $H_q^n(d_h)$, $d_h\in\mathcal{G}$. Unlike the functions G_q, S_q, the coefficients H_q^n are regular at $d=0$ and are well approximated by polynomial functions.

Note that the regular field $(\boldsymbol{u}^0,p^0)$, as well as the values $R_X(d_h)$ and $H_q^n(d_h)$, for $d_h\in\mathcal{G}$, can be computed using any fluid/particle solver.

3. Numerical experiments

3.1. *Four particles configuration*

In order to study the convergence of the singular-regular decomposition method, we consider four particles whose centers are respectively

$$\boldsymbol{r}_1 = 0, \quad \boldsymbol{r}_2 = \boldsymbol{r}_1 + (2+d)\mathbf{e}_{12}, \quad \boldsymbol{r}_3 = \boldsymbol{r}_2 + (2+d)\mathbf{e}_{23}, \quad \boldsymbol{r}_4 = \boldsymbol{r}_3 + (2+d)\mathbf{e}_{34},$$

where $d=0.05$ is the distance between successive particles and the $\mathbf{e}_{ij}$ are unit vectors defined as $\mathbf{e}_{ij} = \boldsymbol{k}_{ij}/k_{ij}$ with

$$\boldsymbol{k}_{12} = (0,\,0,\,1)\,, \quad \boldsymbol{k}_{23} = (0.25,\,0.25,\,1)\,, \quad \boldsymbol{k}_{34} = (0.2,\,-0.1,\,0.75)\,.$$

The boundary conditions $\boldsymbol{v}_i$ are given by the respective velocities and angular velocities:

$$\boldsymbol{U}_1 = (1,\,3,\,2), \quad \boldsymbol{U}_2 = (4,\,2,\,3), \quad \boldsymbol{U}_3 = (3,\,1,\,2), \quad \boldsymbol{U}_4 = (-1,\,-1,\,1),$$

$$\boldsymbol{\omega}_1 = (2,\,0,\,-3), \quad \boldsymbol{\omega}_2 = (-1,\,-2,\,0), \quad \boldsymbol{\omega}_3 = (2,\,1,\,-2), \quad \boldsymbol{\omega}_4 = (-1,\,-1,\,1).$$

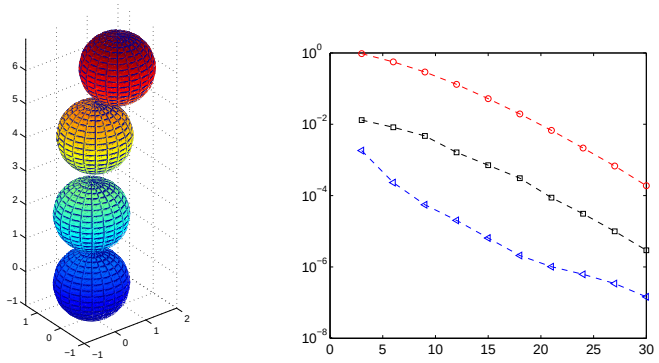

FIGURE 3. The 4 balls configuration (left) and the corresponding relative error versus L for the three methods (right). Direct method ($-\circ-$), Stokesian Dynamics method ($-\square-$) and singular-regular decomposition method ($-\triangleleft-$).

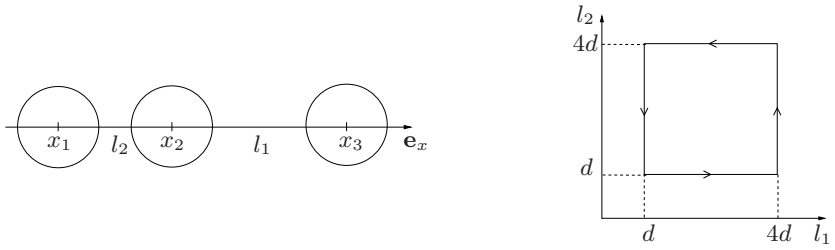

FIGURE 4. 3 balls swimmer: notations (left) and stroke (right)

These configuration and displacements being given, we compute the forces and torques exerted on the four particles $(\boldsymbol{F}_j, \boldsymbol{T}_j)_{j=1\ldots4}$, using the three methods previously mentioned: the direct method, the Stokesian Dynamics correction and the singular-regular decomposition method. For the off-line computations of the last two methods, the truncation order used in the expansions in Vectorial Spherical Harmonic is $L_{\text{off-line}} = 61$. The relative error for each method is represented on Figure 3 as a function of the truncation order L.

3.2. *Three sphere swimmer*

Let us consider the three sphere swimmer described in Najafi & Golestanian (2004). This swimmer is composed of three identical aligned spheres (see Figure 4). The particle i is centered at $\boldsymbol{r}_i = x_i\mathbf{e}_x$, has velocity $\boldsymbol{v}_i = u_i\mathbf{e}_x$ and exerts the force $\boldsymbol{F}_i = F_i\mathbf{e}_x$ on the fluid.

The swimmer is completly described by the position of the central ball x_2 and the lengths l_1, l_2 of the two arms. A stroke is defined as a periodic deformation of the shape of the swimmer which corresponds to a periodic function $s \in [0,1] \to (l_1(s), l_2(s)) \in \mathbf{R}^2$. Such a stroke being given, the question is to compute the corresponding displacement $x_2(1) - x_2(0)$. The swimmer is supposed to be self-propelled so that sum of the forces exerted on the three balls have to be zero:

$$\sum_i F_i(x_1, x_2, x_3, u_1, u_2, u_3) = 0. \tag{3.1}$$

Then, the displacement of the swimmer can be computed by solving (3.1). Note that,

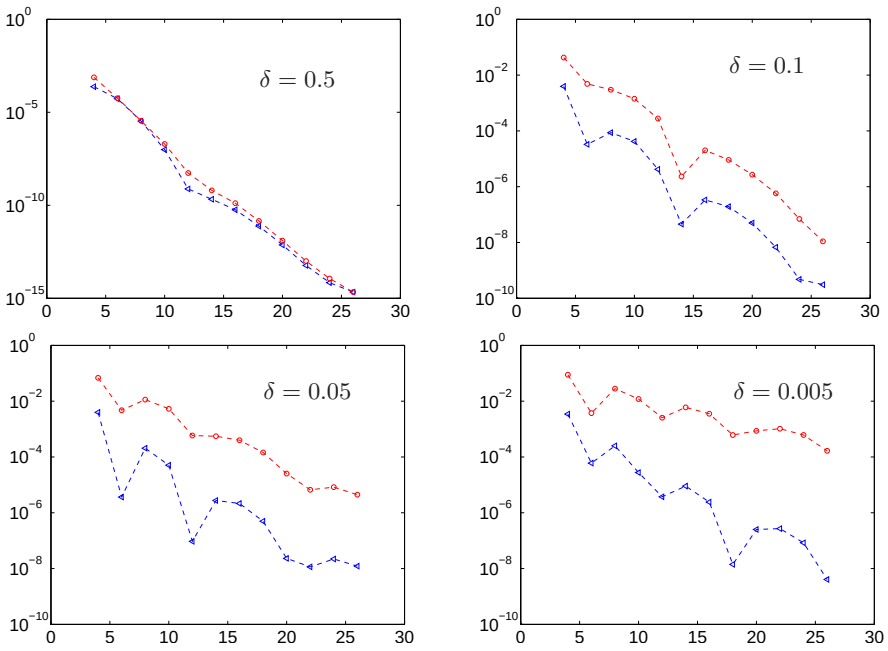

FIGURE 5. 3 balls swimmer: relative error on the displacement of the swimmer versus L for the three methods. Direct and Stokesian Dynamics method ($-\circ-$), and singular-regular decomposition method ($-\triangleleft-$).

since (3.1) only involves the sum of the forces exerted on the three particles, the Stokesian Dynamics correction gives the same results as the direct method.

We consider the square stroke described on Figure 4. We plot on Figure 5 the error for the direct and the singular-regular decomposition methods. The computations are carried out for different values of d. As expected, the smaller d is, the more useful is the singular-regular decomposition method.

REFERENCES

ALOUGES, FRANÇOIS, DESIMONE, ANTONIO, HELTAI, LUCA, LEFEBVRE, ALINE & MERLET, BENOÎT 2013 Optimally swimming stokesian robots. *Discrete Contin. Dyn. Syst. Ser. B* **18** (5), 1189–1215.

ALOUGES, FRANÇOIS, DESIMONE, ANTONIO & LEFEBVRE, ALINE 2008 Optimal strokes for low Reynolds number swimmers: an example. *J. Nonlinear Sci.* **18** (3), 277–302.

BRADY, J.F. & BOSSIS, G. 1988 Stokesian dynamics. *Ann. Rev. Fluid Mech.* **20**, 111–57.

CICHOCKI, B., EKIEL-JEZEWSKA, M.L. & WAJNRYB, E. 1999 Lubrication corrections for three-particle contribution to short-time self diffusion coefficients in colloidal dispersions. *J. Chem. Phys.* **111** (7), 3265–3273.

CICHOCKI, B., FELDERHOF, B. U., HINSEN, K., WAJNRYB, E. & BLAWZDZIEWICZ, J. 1994 Friction and mobility of many spheres in stokes flow. *J. Chem. Phys.* **100**, 3780.

COX, R.G. 1974 The motion of suspended particles almost in contact. *Int. J. Multiphase Flow* **1**, 343–371.

DOUGLAS, SHAWN M., BACHELET, IDO & CHURCH, GEORGE M. 2012 A logic-gated nanorobot for targeted transport of molecular payloads. *Science* **335**, 831–834.

DURLOFSKY, L., BRADY, J.F. & BOSSIS, G. 1987 Dynamic simulation of hydrodynamically interacting particles. *J. Fluid Mech.* **180**, 21–49.

LADD, A.J.C. 1988 Hydrodynamic interactions in a suspension of spherical particles. *J. Chem. Phys.* **88**, 5051.

Lefebvre-Lepot, Aline & Merlet, Benoît 2009 A Stokesian submarine. In *CEMRACS 2008—Modelling and numerical simulation of complex fluids*, *ESAIM Proc.*, vol. 28, pp. 150–161. EDP Sci., Les Ulis.

Najafi, A. & Golestanian, R. 2004 Simple swimmer at low Reynolds number: Three linked spheres. *Phys. Rev. E* **69** (6), 062901.

Patankar, N.A., Singh, P., Joseph, D.D., Glowinski, R. & Pan, T-W. 2000 A new formulations for the distributed lagrange multiplier/fictitious domain method for particulate flows. *Int. J. Multiphase Flow* **26**, 1509–152.

Sangani, A.S. & Mo, G. 1994 Inclusion of lubrication forces in dynamic simulations. *Phys. Fluids* **6**, 1653.

Yeo, K. & Maxey, M.R. 2010 Simulation of concentrated suspensions using the force-coupling method. *J. Comp. Phys.* **229**, 2401–2421.